

Silver nanoparticles incorporated into $\text{Na}_2\text{Ti}_6\text{O}_{13}$ microfibers

V. Rodríguez-González^a, I. Juárez-Ramírez^a, R. Zanella^b, M.E. Zarazúa^a and L.M. Torres-Martínez^{a,*}

^aUniversidad Autónoma de Nuevo León, Facultad de Ingeniería Civil, Instituto de Ingeniería Civil, Depto. de Ecomateriales y Energía, Ave. Universidad S/N, San Nicolás de los Garza, Nuevo León, Mexico Nuevo León C.P. 66451, México

^b Centro de Ciencias Aplicadas y Desarrollo Tecnológico, Universidad Nacional Autónoma de México, Circuito Exterior S/N, Ciudad Universitaria, A. P. 70-186, Delegación Coyoacán, C.P. 04510, México D. F., Mexico

This research is concerned with novel semiconductor composites of sodium hexatitanate oxide ($\text{Na}_2\text{Ti}_6\text{O}_{13}$), and silver metallic nanoparticles. The $\text{Na}_2\text{Ti}_6\text{O}_{13}$ was prepared by two methods, a sol-gel process and a solid state reaction. The silver nanoparticles were incorporated into the titanate by a deposition-precipitation technique, using NaOH as precipitation agent in the dark. $\text{Ag}/\text{Na}_2\text{Ti}_6\text{O}_{13}$ microfibers were obtained by the sol-gel method, meanwhile octagonal microbar agglomerates were the product of the solid state reaction. The SEM-TEM observations showed silver particles with a nanometric size (5-7 nm); and fibrillar structures in the sol-gel sodium titanates. The UV-Vis-RD spectroscopy showed a blue shift Eg from 3.3 to 3.4 nm; and a plasmon surface resonance in the visible region. These materials are proposed as potential photocatalysts for contaminated water purification.

Key words: Solid state sodium titanates, Sol-gel microfiber synthesis, $\text{Na}_2\text{Ti}_6\text{O}_{13}$ microfibers, Silver decorated nanofibers, Silver Surface Plasmon Resonance.

Introduction

Alkali titanates are of great interest because of possible applications such as for photocatalysts [1-3], fuel cell electrolytes [4], and cation exchangers [5] for the treatment of radioactive liquid waste. As for sodium hexatitanate ($\text{Na}_2\text{Ti}_6\text{O}_{13}$), it has been used as an ionic exchanger, a gas sensor as well as in ceramic capacitors [6, 7]. Sodium hexatitanate ($\text{Na}_2\text{Ti}_6\text{O}_{13}$) belongs to the alkali titanate family with a formula $\text{A}_2\text{Ti}_n\text{O}_{2n+1}$. Its structure consists of octahedral TiO_6 , edge-shared and corner-shared, forming rectangular tunnels. The alkali titanates have shown important activity for water splitting [1, 8, 9]. In addition the phase $\text{Na}_2\text{Ti}_6\text{O}_{13}$ has been reported as a photocatalyst for the 2,4-dinitroaniline degradation reaction [10, 11]. In the present study, the characterization by nitrogen adsorption, X-ray Diffraction (XRD), Scanning Electron Microscopy (SEM), Transmission Electron Microscopy (TEM), UV-Vis and Raman spectroscopy of silver sodium hexatitanate prepared by both a sol-gel and solid state techniques is reported.

Experimental

The sodium hexatitanate ($\text{Na}_2\text{Ti}_6\text{O}_{13}$) was prepared by a sol-gel method and by a solid state reaction as follows:

for the sol-gel synthesis, 0.11 mol of titanium isopropoxide (Aldrich 99.99%) was added drop by drop to a solution containing 0.70 mol of distilled water, 104.5 mol of ethanol (DEQ 99%) and 0.036 mol of sodium acetate (Aldrich 99%). When the addition of titanium isopropoxide was finished, the pH of the solution was adjusted to 9 using ammonium hydroxide (25-28% vol, DEQ). Then, the gelling solution was refluxed for 3 days at 70 °C under constant stirring. Afterwards, the fresh materials were dried at 100 °C; and then annealed at 750 °C for 72 h. The solid state reaction was performed by mixing Na_2CO_3 (Aldrich 99%) and TiO_2 (Aldrich 99.8%) taking into account the required stoichiometry. The solid solution was placed into an electric oven; and then annealed in air at 950 °C for 32 h, using a 1 K cm^{-1} heating rate. The silver nanoparticles were deposited using a NaOH deposition-precipitation method. The annealed sodium hexatitanate ($\text{Na}_2\text{Ti}_6\text{O}_{13}$) was dispersed in 13 ml of an aqueous solution containing an adequate quantity of AgNO_3 (7.42×10^{-3} M) to obtain a final load of 1.0 wt% of Ag in the titanate. The solution was heated at 80 °C; and then, a solution of NaOH (0.5 M) was added until a pH of 9 was reached, promoting the precipitation of AgOH on the titanate. The synthesis processes were performed with vigorous stirring in the dark to avoid the decomposition of the silver precursor due to light. After the silver deposition on the titanates, the solids were separated from the silver solution by centrifugation. Then, the solids were washed several times with warm distilled water (50 °C); and dried under vacuum for 2 h at 90 °C. Finally, the solids were reduced with a hydrogen flow

*Corresponding author:
Tel : 00528183321902 ext 112
Fax: 00528183321902 ext 106
E-mail: letorre@fic.uanl.mx

(500 ml/minute) at 200 °C for 2 h in a U glass reactor equipped with a fritted plate with a diameter of 1.5 cm. All the samples were stored at room temperature in a vacuum desiccator, in the dark, in order to prevent light-induced modifications. The silver semiconductors were labeled as Ag/NaTSG and Ag/NaTSS, where NaTSG denotes the sodium titanate prepared by the sol-gel method; and NaTSS that prepared by the solid state reaction.

Characterization of silver $\text{Na}_2\text{Ti}_6\text{O}_{13}$ nanofibers

The powder XRD patterns of the stabilized samples were recorded at room temperature on a Bruker D8 Advance diffractometer using $\text{CuK}\alpha$ radiation (with 2θ ranging from 10° to 70°). The specific surface area of the solids was measured by nitrogen adsorption at -196°C using a Quantachrome 3B automatic instrument. The specific surface area was calculated using the Brunauer-Emmett-Teller method (BET method). Before the nitrogen adsorption, the catalyst was out-gassed at 350°C for 12 h to remove adsorbed impurities. The UV-Vis spectra (200-900 nm) of the solids were obtained with a Perkin-Elmer spectrophotometer; model Lambda 35 (diffuse reflectance mode). The band gap of the solids was calculated by linearization of the slope to the X axis (wavelength, nm) for Y axis (absorbance) equal to zero. Scanning electron microscopy (SEM) observations were performed with a JEOL 6490 LV electron microscope using semiquantitative energy dispersive X ray spectroscopy (EDS). The thermally treated samples were also examined by TEM in a 2010 FasTem analytical microscope equipped with a Z-contrast annular detector. The powder samples were dispersed in water and supported on holey carbon coated copper grids. High resolution transmission electron microscopy (HRTEM) and high angle annular dark field (HAADF) digital images were obtained using Digital Micrograph Software from GATANTM. The histograms of the metal particle sizes were obtained from measuring about 400-500 particles. The size limit for the detection of silver particles was 1 nm. The particle average diameter was calculated from the following formula: $= \frac{\sum ni di}{\sum ni}$, where (ni) is the number of particles with diameter (di). The Raman spectra were recorded on a Nicolet Almega Dispersive Raman Spectrometer, equipped with an NdYVO₄ laser source. The laser excitation line was 532 nm; and the power was of 25 mW.

Results and Discussion

The XRD patterns of the solids are shown in Fig 1: (a) In the starting sodium titanate semiconductors, the sodium hexatitanate phase, $\text{Na}_2\text{Ti}_6\text{O}_{13}$ (JCPDF 73-1398), was identified; (b) The starting $\text{Na}_2\text{Ti}_6\text{O}_{13}$ and silver decorated nanofibers synthesized by the DP method show identical patterns; (c) Neither the XRD peaks of the silver particles nor a change (shift or less intensity) of the XRD peaks of $\text{Na}_2\text{Ti}_6\text{O}_{13}$ could be observed. The fact that the XRD

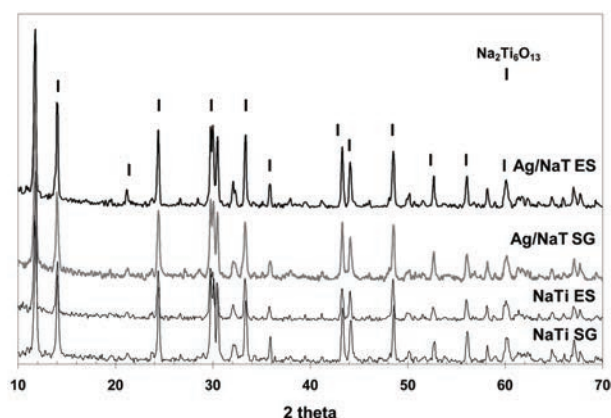


Fig. 1. XRD patterns for silver incorporated into sodium titanates and sodium titanates.

Table 1. Textural and semiconductor properties of silver-sodium titanates

Titanate	S_{BET} (m^2/g)	E_g (eV)	SPR* (nm)
$\text{Na}_2\text{Ti}_6\text{O}_{13}$ SG	< 10	3.26	-
$\text{Na}_2\text{Ti}_6\text{O}_{13}$ ES	< 10	3.30	-
Ag/ $\text{Na}_2\text{Ti}_6\text{O}_{13}$ SG	< 10	3.44	551
Ag/ $\text{Na}_2\text{Ti}_6\text{O}_{13}$ ES	< 10	3.38	549

* Surface Plasmon Resonance absorption.

silver peaks cannot be identified, could be due either to its low content (1 wt %) or to the nanosized silver particles, which are not detectable by XRD. The specific surface area obtained on both samples was $10 \text{ m}^2/\text{g}$ (Table 1). These results show that the impregnation of the samples with silver nitrate does not modify the textural properties of the sodium titanate. The BET values correspond to the same interval order reported in the literature for alkali titanates [11]. The morphology of the titanate and of the silver decorated titanate was analyzed by SEM. In Fig. 2, the SEM images obtained for the AgNaTSG and NaTSG samples, are shown. The SEM pictures show the formation of fibers in both samples with a typical diameter of 0.10-0.20 μm ; and a length of around 5 μm . On the other hand, in Fig. 3, the morphology of the sodium hexatitanate prepared by the solid state reaction, is shown. In such samples the formation of microbars instead of microfibers may be observed. It can also be noted that in the silver-containing samples, the contrast in the images becomes

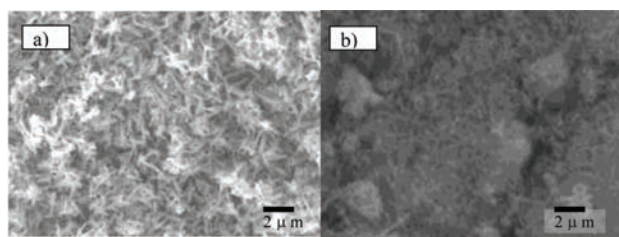


Fig. 2. SEM images for: (a) sol-gel sodium hexatitanate; (b) sol-gel-silver-decorated sodium titanate.

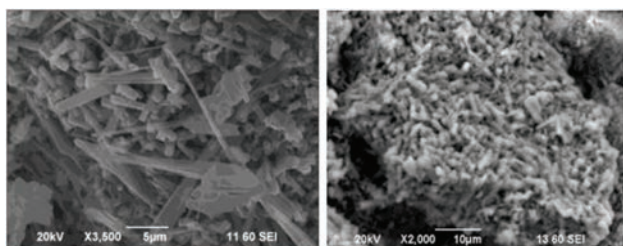


Fig. 3. SEM images for: (a) solid state sodium hexatitanate; and (b) solid-state-silver decorated sodium titanate.

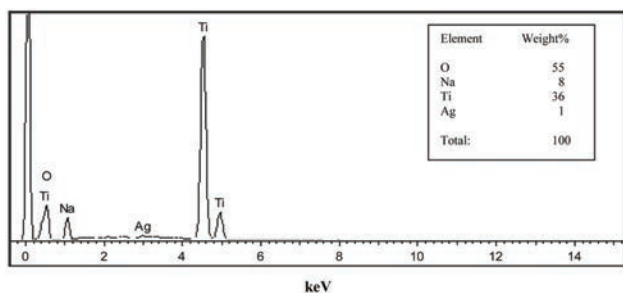


Fig. 4. Selected EDS spectra with the elemental analysis for the silver semiconductors.

darker. During the SEM analysis, the images were obtained without distortion due to a silver-surface-conduction phenomenon. In Fig. 4, the selected EDS spectrum with the elemental analysis for the silver-containing titanates is shown. The average values are close to that of the nominal composition for both preparations. It seems that the DP method with NaOH is a good technique to obtain highly dispersed silver particles. In order to determine the size of the silver particles, TEM studies were performed. Fig. 5 shows an HAADF-STEM picture of the silver titanate prepared by the sol-gel method. Microfiber formation

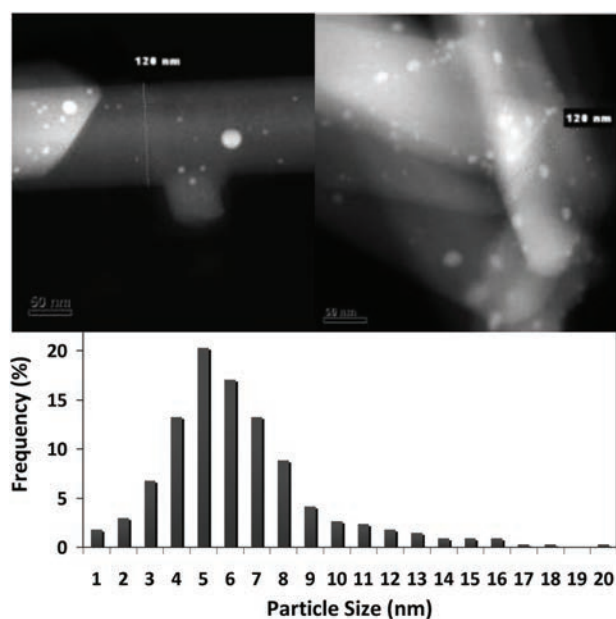


Fig. 5. TEM image in Z contrast and HRTEM for the Ag/NaTSG semiconductor.

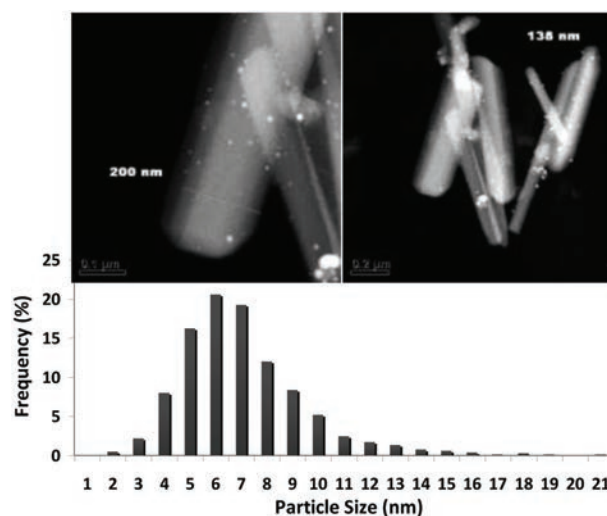


Fig. 6. TEM image in Z contrast and HRTEM for the Ag/NaTSS semiconductor.

as well as the silver nanoparticles may be observed. To improve the accuracy of the determination of the sizes of the silver particles, the samples were analyzed by HAADF-STEM (high-angle annular dark-field scanning transmission electron microscopy) using a 2010 FasTem analytical microscope. The selected image shows a microfiber sample with a diameter of $0.12\ \mu\text{m}$; and a range of silver nanoparticles. In the HAADF-STEM image, the corresponding silver particle size distribution has been inserted. The average silver particle size for the sol-gel material was $5.5\ \text{nm}$. On the other hand, in Fig. 6, the HAADF-STEM picture for the solid state preparation is shown. Octagonal microbar agglomerates of sodium titanates and with different lengths, can be seen. In this case, the silver average particle size was $6.4\ \text{nm}$. The production of fibril structures of sodium hexatitanates strongly depends on the preparation method; and the sol-gel method was the correct technique to obtain microfibers. Analogous $\text{Na}_2\text{Ti}_3\text{O}_7$ structures have been prepared by a sol-gel method, showing micro-pellets like those that we obtained by the solid state technique for the $\text{Na}_2\text{Ti}_6\text{O}_{13}$ [12]. The most similar fibril morphology to that obtained in the present work was reported by Song et al. [13]. They prepared $\text{Na}_2\text{Ti}_3\text{O}_7$ by a hydrothermal method. Thin fiber titanates with a diameter of $50\ \text{nm}$ and lengths up to several micrometres were reported [14]. Very thin nanowires, have been synthesized by treating brookite and anatase nanocrystallites in a NaOH aqueous solution under hydrothermal conditions [14]. Fig. 7 shows the UV-Vis diffuse reflectance spectra of: (a) sodium hexatitanate prepared by the sol-gel method; and by the solid state reaction; (b) silver decorated $\text{Na}_2\text{Ti}_6\text{O}_{13}$ nanofibers. This figure clearly demonstrates that the absorption edge shifted to a lower wavelength with the incorporation of silver nanoparticles from 3.26 to 3.44 (Table 1). In the visible region of the spectra, a surface plasmon resonance (SPR) was observed in the silver semiconductors at $549\ \text{nm}$ for Ag/NaTSE; and $551\ \text{nm}$

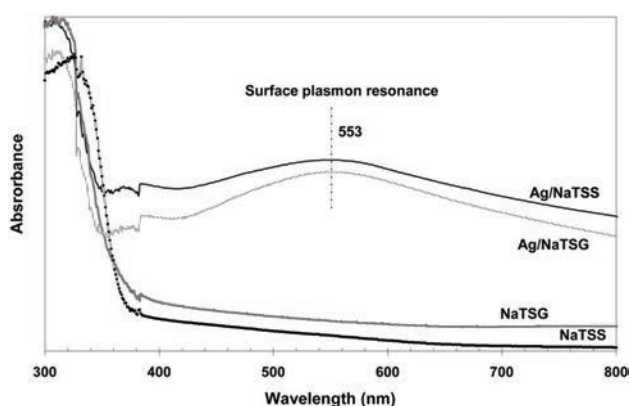


Fig. 7. UV-Visible spectra of sodium hexatitanates before and after the incorporation of silver nanoparticles.

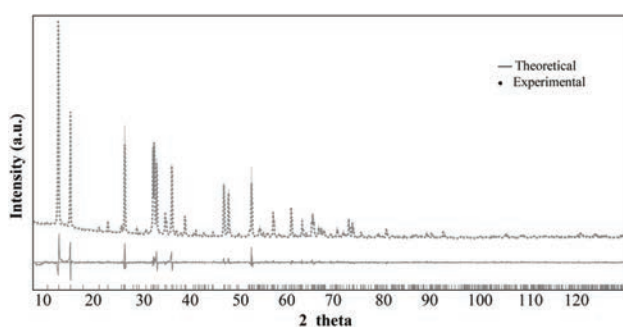


Fig. 8. Rietveld refinement of silver-solid hexatitanate prepared by the solid state reaction.

for the Ag/NaTSG samples. Such a SPR absorption has also been reported for silver nanoparticles on different SiO_2 -based substrates (soda-lime glass, quartz glass and mesoporous SiO_2) [15]. The SPR can be explained by the silver size effect; a plasmon absorption was observed for particles bigger than 5 nm [16]. In gold nanoparticles prepared by a similar method on different supports, the plasmon absorption was observed when the gold particles grew on the supports with a low specific surface area [17]. It is assumed in the present study that the low specific surface area of the sodium titanates favors the formation of silver nanoparticles bigger than 5 nm, which are responsible for the observed plasmon. The Rietveld refinement was performed on the XRD patterns in order to elucidate if the incorporation of silver nanoparticles into the surface microfibers distorted the sodium hexatitanate framework. Fig. 8 shows the XRD patterns refined by the Rietveld method for the Ag/NaTSS solid. No differences in the pattern form that of JCPDF 73-1398 may be seen. The

Table 2. Cell parameters calculated by the Rietveld Method for Ag- $\text{Na}_2\text{Ti}_6\text{O}_{13}$ prepared by the sol gel and solid state reaction methods

Sample	Cell Parameters			
	a (Å)	b (Å)	c (Å)	Volume (Å ³)
Ag/ $\text{Na}_2\text{Ti}_6\text{O}_{13}$ SG	15.09577(3)	3.74531(5)	9.17406(3)	512.284
Ag/ $\text{Na}_2\text{Ti}_6\text{O}_{13}$ ES	15.10834(4)	3.74725(5)	9.17551(8)	513.059

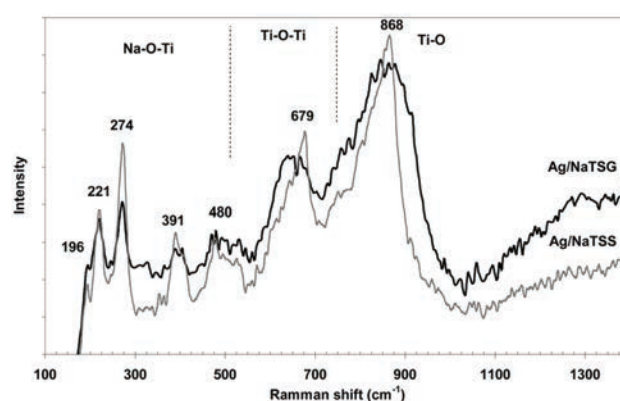


Fig. 9. Raman spectra of the samples after silver incorporation.

silver particles must be anchored on the surface of the sodium titanate without modification of the framework, (Table 2) where it is shown that the cell parameters obtained by the Rietveld method for Ag- $\text{Na}_2\text{Ti}_6\text{O}_{13}$ prepared by sol gel and solid state reaction; only a loss in the intensity of the peaks was observed. The tunnel structure of sodium hexatitanate crystallizes in the monoclinic system, C12/m space group. Finally, we studied the structural differences of the silver titanates by Raman spectroscopy. The Raman spectra for the Ag/NaTSG and Ag/NaTSS samples are shown in Fig 9. The spectra are very similar in both samples, only small differences in the band intensities are observed. The identification of the peaks was as follows: the peak at 176 cm^{-1} denotes the Na-O-Ti stretching vibration in the titanate structure; the peaks at about 221 and 278 cm^{-1} correspond to Na-O-Ti bonds, meanwhile the peaks at about 679 and 868 cm^{-1} are assigned to the Ti-O-Ti stretching vibration in edge-shared TiO_6 ; and the peak near 920 cm^{-1} was reported for a short Ti-O stretching vibration in distorted TiO_6 [14]. The main difference is the intensity of the bands in the Na-O-Ti region; there are more intense bands for the solid state preparation samples in comparison with the sol-gel samples. The sharpness of the bands is related to the crystallinity of the sodium titanates; usually the solid state preparation produces highly crystalline solids. These results are in good agreement with those obtained by XRD. The low silver content (1 wt%) does not permit one to observe any modification in the Raman spectra. The fibril-sol-gel-silver-decorated titanates could be useful for the photocatalytic purification of contaminated water due to the antibacterial properties of silver nanoparticles under UV-Vis irradiation.

Conclusions

The main conclusions of the present study are the following: i) when the sodium hexatitanate oxide ($\text{Na}_2\text{Ti}_6\text{O}_{13}$) was prepared by a sol-gel method, the formation of solids with a fibril morphology was obtained (cylindrical microfiber $0.2\text{ }\mu\text{m} \times 5\text{ }\mu\text{m}$); as for the solid state reaction, octagonal microbar agglomerates were formed; ii) a

few silver nanoparticle agglomerates were found on the microfiber surface; iii) HAADF-STEM elemental mapping Z contrast observations showed the formation of surface silver nanoparticles ($d \sim 5\text{-}7$ nm); iv) the incorporation of silver into the titanates modified the semiconductivity of the solids; a band-gap blue shift to 3.4 eV was observed; a surface plasmon resonance was observed in the visible region. The fibril morphology of the silver titanates obtained by the sol-gel method as well as the modifications in the semiconductivity properties enable us to propose these new semiconductors as potential antibacterial materials for the photocatalytic antibacterial purification of water.

Acknowledgements

UANL-PAICYT 2007 projects CA 1507-07 AND 1522-07, PROMEP 103.5/07/3578, and 103.5/08/3125. Also we thank Karina Del Angel for the synthesis help; and the technical assistance provided by Luis Rendón (LCM-IF, HRTEM), Viridiana Maturano (Raman), Miguel A. Ruiz Gómez (SEM-DRX); and Xiomara L. García Montelongo

References

1. M.A. Peña and J.L.G. Fierro, *Chem. Rev.* 101 (2001) 1981-2017.
2. Z. Zou and H. Arakawa, *J. Photochem. Photobiol. A: Chem.* 158 (2003) 145-162.
3. J.H. Choy, H.C. Lee, H. Jung and S.J. Huang, *J. Mater. Chem.* 11 (2001) 2232-2237.
4. D.J.D. Corcoran, D.P. Tunstall and J.T.S. Irvine, *Solid State Ionics* (2000) 136-137, 297-303.
5. I.M. El-Naggar, E.A. Mowafy, I.M. Ali and H.F. Aly, *Adsorption* 8[3] (2002) 225-234 (10).
6. P. Szlivia and K. Laszló; *J. Solid State Chem.* 178 (2005) 1614-1619.
7. C.-X. Xu, Q. Zhang and H. Zhang; *J. Am. Chem. Soc.* 127 (2005) 11583-11585.
8. S. Ikeda, K. Hirao, S. Ishino, M. Matsumura and B. Ohtani, *Catal Today*, 117 (2006) 343-349.
9. M. Machida, X. Wei Ma, H. Taniguchi, J.-I Yabunaka and T. Kijima, *J. Mol. Catal. A: Chemical*, 155 (2000) 131-142.
10. L.M. Torres-Martínez, A. Hernández and J.C. Luna-Urzúa. *Adv. Tech. Matls. Matls. Proc. J. (ATM)*. 6 (2004)184-191.
11. A. Hernández, L.M. Torres-Martínez, W. Ortega and T. López. *Emerging Fields in Sol-gel Science and Technology*. Kluwer Academy Publishers 2003, pp. 84-91, Boston. Hardbound ISBN-1-4020-7458-1.
12. A-L. Sauvet, S. Baliteau, C. Lopez and P. Fabry; *J. Solid State Chem.* 177 (2004) 4508-4515.
13. H. Song, H. Jiang, T. Liu, X. Liu and G. Meng; *Materials Research Bull.* 42 (2007) 334-344.
14. X.D. Meng, D.-Z. Wanga, J-H. Liua and S.-Y Zhang; *Materials Research Bulletin* 39 (2004) 2163-2170, and references therein.
15. J. Hu, W. Cai1, H. Zeng, C. Li and F. Sun, *J. Phys.: Condens. Matter* 18 (2006) 5415-5423.
16. P.V. Kamat, *J. Phys. Chem. B* 106 (2002) 7729-7744.
17. V. Rodríguez-González, R. Zanella, G. del Ángel and R. Gómez, *J. Mol. Catal. A: Chemical*, 281 (2008) 93-98.